

Dressed symbolic dynamics

Robert Gilmore¹ and Christophe Letellier²

¹*Physics Department, Drexel University, Philadelphia, Pennsylvania 19104*

²*CORIA UMR 6614, Université de Rouen, Avenue de l'Université, Boîte Postale 12, F-76801 Saint-Etienne du Rouvray cedex, France*

(Received 4 October 2002; published 24 March 2003)

A strange attractor (SA) with symmetry group \mathcal{G} can be mapped down to an image strange attractor SA without symmetry by a smooth mapping with singularities. The image SA can be lifted to many distinct structurally stable strange attractors, each equivariant under \mathcal{G} , all with the same image SA. If the symbolic dynamics of the image SA requires s symbols $\sigma_1, \sigma_2, \dots, \sigma_s$, then $|\mathcal{G}|^s$ symbols are required for symbolic dynamics in the covers, and there are $|\mathcal{G}|^s$ distinct equivariant covers. The covers are distinguished by an index. The index is an assignment of a group operator to each symbol $\sigma_i: \sigma_i \rightarrow g_{\alpha_i}$. The subgroup $\mathcal{H} \subset \mathcal{G}$ generated by the group operators g_{α_i} in the index determines how many disconnected components ($|\mathcal{G}|/|\mathcal{H}|$) each equivariant cover has. The components are labeled by coset representatives from \mathcal{G}/\mathcal{H} . The structure of each connected component is determined by \mathcal{H} . A simple algorithm is presented for determining the number and the period of orbits in an equivariant attractor that cover an orbit of period p in the image attractor. Modifications of these results for structurally unstable covers are summarized by an adjacency diagram.

DOI: 10.1103/PhysRevE.67.036205

PACS number(s): 05.45.-a

I. INTRODUCTION

Many physical systems exhibit a symmetry. These include quantum systems that are invariant under complex conjugation [$\Psi(\mathbf{x}, t) \rightarrow \Psi^*(\mathbf{x}, t)$], electromagnetic systems that are invariant under field reversal [$\mathbf{E}(\mathbf{x}, t) \rightarrow -\mathbf{E}(\mathbf{x}, t)$], and fluid systems that are unchanged under reversals of the velocity vector field [$\mathbf{u}(\mathbf{x}, t) \rightarrow -\mathbf{u}(\mathbf{x}, t)$]. Three of the four most studied three-dimensional systems are truncations of electromagnetic (Duffing, van der Pol) or fluid (Lorenz) models, and exhibit twofold symmetries.

When particular variables are monitored, for example, the probability $P(\mathbf{x}, t) = |\Psi(\mathbf{x}, t)|^2$ or the intensity $I(\mathbf{x}, t) = \mathbf{E}(\mathbf{x}, t) \cdot \mathbf{E}(\mathbf{x}, t)$, information about the symmetry is lost. If the dynamics is chaotic, then the strange attractor reconstructed from these observables will have a lower symmetry than a strange attractor reconstructed from the most fundamental variables [e.g., $\Psi(\mathbf{x}, t), \mathbf{E}(\mathbf{x}, t)$] [1,2]. For example, the strange attractor constructed from the Z variable of the Lorenz dynamical system is a $2 \rightarrow 1$ image of strange attractors constructed from either the X or Y variable [3]. Similar statements hold for strange attractors constructed from variables in the van der Pol (rotating) plane of either the Duffing or van der Pol oscillators, compared with strange attractors constructed from the X or Y variable intrinsic to these two driven dynamical systems [4].

It is important to understand the spectrum of strange attractors, with a given symmetry, that is compatible with an observed attractor with lower symmetry or no symmetry at all. It is a surprising result that many different strange attractors, all with the same symmetry, are compatible with an observed strange attractor with lower symmetry. By “compatible” we mean that the attractors with and without symmetry are related by a local diffeomorphism with the specified symmetry. When the symmetry involves a rotation axis, the different strange attractors, all with the same rotation symmetry, that cover a particular image attractor (without symmetry) are distinguished by topological indices [1].

In this work, we show that the inequivalent covers of an image dynamical system are distinguished among themselves by a set of indices. The indices are the operations of the symmetry group. Each symbol encoding an orbit in the image attractor is assigned an index (group label). Each different assignment corresponds to a different covering attractor. All covering attractors possess the same symmetry. We illustrate these ideas by applications to two different symmetry groups with four group elements acting in three-dimensional phase spaces. Extensions to other symmetry groups, both commutative and noncommutative, and to higher-dimensional phase spaces, are straightforward.

In Sec. II, we introduce these two groups and discuss their action in \mathbb{R}^3 . In Sec. III we describe how they are used to decompose the phase space into symmetry-related domains, each identified by a group element. In Sec. IV, we describe the properties of the dynamical system equations for the cover and image dynamical systems. Cover and image attractors are characterized by their branched manifolds in Sec. V, and the scheme for indexing the covering attractors is introduced in Sec. VI. The spectrum of covering attractors for the two symmetry groups is presented and described in Sec. VII. We describe structurally unstable covering attractors in Sec. VIII. Finally, we conclude with a number of remarks and observations.

II. GROUPS

At the abstract level there is one group of order two, one group of order three, and two groups of order four. The group of order two has one generator A and obeys the relation $A^2 = \mathbb{I}$. The group of order three has one generator A and obeys the relation $A^3 = \mathbb{I}$. One of the two order-four groups has one generator A that obeys $A^4 = \mathbb{I}$. The other order-four group has two generators A and B , and obeys the three relations $A^2 = B^2 = \mathbb{I}$ and $AB = BA$ [5].

The group of order two has three different inequivalent faithful representations in the three-dimensional phase space

\mathbb{R}^3 . The generators have matrix representations

$$\begin{array}{ccc} \sigma_Z & R_Z(\pi) & \mathcal{P} \\ \begin{bmatrix} 1 & 0 & 0 \\ 0 & 1 & 0 \\ 0 & 0 & -1 \end{bmatrix} & \begin{bmatrix} -1 & 0 & 0 \\ 0 & -1 & 0 \\ 0 & 0 & +1 \end{bmatrix} & \begin{bmatrix} -1 & 0 & 0 \\ 0 & -1 & 0 \\ 0 & 0 & -1 \end{bmatrix} \end{array}$$

These generators describe the group of reflections in the X - Y plane $Z=0$ (σ_Z), rotations through π radians about the Z axis [$\mathcal{R}_Z(\pi)$], and spatial inversions (\mathcal{P}). The operator σ_Z leaves invariant the X - Y plane $Z=0$. As a result, any double cover with σ_Z symmetry must be disconnected, with one component in the upper half space $Z>0$ and the mirror image in the lower half space $Z<0$. By contrast, the invariant set of $R_Z(\pi)$ is one dimensional (Z axis) and that of \mathcal{P} is zero dimensional (the origin). These lower-dimensional invariant sets do not provide any obstructions to connected covers with $R_Z(\pi)$ symmetry or \mathcal{P} symmetry [1].

The unique order-three group has a single faithful representation in \mathbb{R}^3 . The generator A describes a rotation by $2\pi/3$ radians about the Z axis.

The cyclic order-four group A ($A^4=\mathbb{I}$) has two faithful representations in \mathbb{R}^3 , \mathcal{C}_4 and \mathcal{S}_4 , whose generators are given by

$$C_4 = \begin{bmatrix} 0 & 1 & 0 \\ -1 & 0 & 0 \\ 0 & 0 & 1 \end{bmatrix},$$

$$S_4 = \sigma_Z C_4 = \begin{bmatrix} 0 & 1 & 0 \\ -1 & 0 & 0 \\ 0 & 0 & -1 \end{bmatrix}.$$

The generator C_4 describes rotations by $2\pi/4$ radians about the Z axis and $C_4^4=\mathbb{I}$. The generator S_4 describes rotations by $2\pi/4$ radians about the Z axis, followed by reflection in the $Z=0$ plane: $S_4^4=\mathbb{I}$. We treat below only the first of these two representations.

For the other abstract four-element group \mathcal{V}_4 (Vier gruppe), the three group operations A, B, AB , represent rotations by π radians about the X, Y , and Z axes. The matrix representations of these operators are

$$\begin{array}{ccc} A=R_X(\pi) & B=R_Y(\pi) & AB=R_Z(\pi) \\ \begin{bmatrix} +1 & 0 & 0 \\ 0 & -1 & 0 \\ 0 & 0 & -1 \end{bmatrix} & \begin{bmatrix} -1 & 0 & 0 \\ 0 & +1 & 0 \\ 0 & 0 & -1 \end{bmatrix} & \begin{bmatrix} -1 & 0 & 0 \\ 0 & -1 & 0 \\ 0 & 0 & +1 \end{bmatrix} \end{array}$$

The invariant set is the union of the three rotation axes. This does not provide an obstruction to the connectedness of the covering attractor. As a result, fourfold covers of an image attractor may have a single component, two distinct symmetry-related covers, or four disjoint covers, each identical to the image attractor. Four-group action of this type has been observed in a fluid model [6].

Since the two groups are Abelian, the group multiplication properties are summarized by their character tables [5]:

\mathcal{C}_4	\mathbb{I}	C_4	C_4^2	C_4^3	Basis vectors
Γ^1	1	1	1	1	$1, Z, X^2+Y^2, X^4-6X^2Y^2+Y^4, 4X^3Y-4XY^3$
Γ^2	1	i	-1	$-i$	$X+iY, (X-iY)^3$
Γ^3	1	-1	1	-1	X^2-Y^2, XY
Γ^4	1	$-i$	-1	i	$X-iY, (X+iY)^3$

\mathcal{V}_4	\mathbb{I}	R_X	R_Y	R_Z	Basis vectors
Γ^1	1	1	1	1	$1, X^2, Y^2, Z^2, XYZ$
Γ^2	1	1	-1	-1	X, YZ
Γ^3	1	-1	1	-1	Y, ZX
Γ^4	1	-1	-1	1	Z, XY

For the two cases, the basis vectors for the irreducible representations are listed. In particular, (a) the basis vectors for the identity representation $\Gamma^{(1)}$ are the fundamental invariant polynomials; (b) the basis vectors for the other representations are the appropriate variables for the equivariant dynamical system equations.

III. SPATIAL DOMAINS

The three-dimensional phase space $\mathbb{R}^3(X, Y, Z)$, in which the equivariant dynamics occurs, can be partitioned into $|\mathcal{G}|$ symmetry-related domains. Each domain is mapped onto another by one of the symmetry group operations. It is possible to identify one domain (the fundamental domain) with the identity group operation. Then each of the other domains can be labeled by a different group operation. Each of the $|\mathcal{G}|$ symmetry-related domains in $\mathbb{R}^3(X, Y, Z)$ is mapped in a one-to-one way onto the phase space $\mathbb{R}^3(u_1, u_2, u_3)$ that supports the image dynamics.

The group \mathcal{C}_4 is distinguished by its rotation (Z) axis. It is useful to choose the fundamental domain as the union of the two octants $(+++)\cup(+-)$, where, for example, $(+-)$ means the set of points $X>0, Y>0, Z<0$. The remaining three domains are obtained from this domain by the action of the three remaining group operations C_4, C_4^2, C_4^3 on the fundamental domain:

Domain label	Domain
\mathbb{I}	$(+++)\cup(+-)$
$C_4=R_Z\left(\frac{\pi}{2}\right)$	$(-++)\cup(-+-)$
$C_4^2=R_Z(\pi)$	$(--+)\cup(---)$
$C_4^3=R_Z\left(\frac{3\pi}{2}\right)$	$(+-+)\cup(+--)$

The group \mathcal{V}_4 is distinguished by three mutually perpendicular rotation axes. These are equivalent under the group \mathcal{C}_3 generated by rotations about the $(1,1,1)$ axis through $2\pi/3$ radians. As a result, the decomposition into domains must

show an appropriate symmetry among the domains labeled by the three rotations. For these reasons, we choose as the fundamental domain the noncontiguous union $(+++)\cup(---)$. The domain decomposition for \mathcal{V}_4 is

Domain label	Domain
I	$(+++)\cup(---)$
$R_X(\pi)$	$(+--)\cup(-++)$
$R_Y(\pi)$	$(-+-)\cup(+ - +)$
$R_Z(\pi)$	$(--+)\cup(++-)$

For later purposes, when we discuss structurally unstable covers, it is useful to know which domains are adjacent. Two domains are adjacent when they share a two-dimensional surface [e.g., $(+++)$ is adjacent to $(-++)$]. This information can be summarized by an adjacency diagram. In such a diagram, each domain is represented by a small circle that is labeled by a group operation. Adjacency between two domains is indicated by connecting the circles representing the domains. The adjacency diagrams for \mathcal{C}_4 and \mathcal{V}_4 are presented in Fig. 1.

Individual group operations act to permute the domains among themselves in a way unique to each group operation. As a result, the domains (their group labels) serve to provide

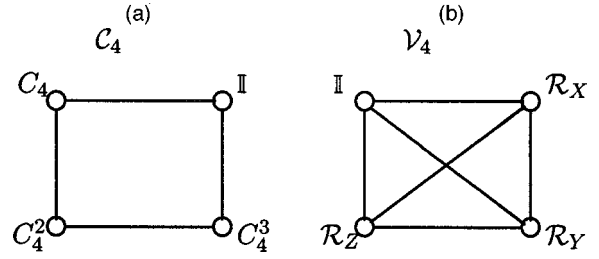


FIG. 1. Adjacency diagrams for the four domains in $\mathbb{R}^3(X, Y, Z)$ under the group (a) \mathcal{C}_4 and (b) \mathcal{V}_4 .

a basis set for a faithful $|\mathcal{G}| \times |\mathcal{G}|$ representation of the group. This is just the regular representation [5] described as

$$g_\alpha g_i = g_j \Gamma_{ji}^{\text{Reg}}(g_\alpha),$$

where

$$\Gamma_{ji}^{\text{Reg}}(g_\alpha) = \begin{cases} 0 & \text{if } g_j \neq g_\alpha g_i \\ 1 & \text{if } g_j = g_\alpha g_i. \end{cases}$$

For \mathcal{V}_4 , the 4×4 matrix representatives of the four group operations are

$$\begin{matrix} & \text{I} & R_X & R_Y & R_Z \\ \text{I} & \begin{bmatrix} 1 & 0 & 0 & 0 \\ 0 & 1 & 0 & 0 \\ 0 & 0 & 1 & 0 \\ 0 & 0 & 0 & 1 \end{bmatrix} & \begin{bmatrix} 0 & 1 & 0 & 0 \\ 1 & 0 & 0 & 0 \\ 0 & 0 & 0 & 1 \\ 0 & 0 & 1 & 0 \end{bmatrix} & \begin{bmatrix} 0 & 0 & 1 & 0 \\ 0 & 0 & 0 & 1 \\ 1 & 0 & 0 & 0 \\ 0 & 1 & 0 & 0 \end{bmatrix} & \begin{bmatrix} 0 & 0 & 0 & 1 \\ 0 & 0 & 1 & 0 \\ 0 & 1 & 0 & 0 \\ 1 & 0 & 0 & 0 \end{bmatrix} \\ R_X & & & & \\ R_Y & & & & \\ R_Z & & & & \end{matrix}$$

IV. EQUIVARIANT AND INVARIANT EQUATIONS

The equations describing a dynamical system with symmetry group \mathcal{G} must be unchanged (equivariant) under the operations of \mathcal{G} . To this end, not all of the basic variables X, Y, Z can be basis vectors for the identity representation $\Gamma^{(1)}(\mathcal{G})$.

For the group \mathcal{C}_4 , Z transforms under the identity representation, but the linear combinations $X \pm iY$ do not. The equivariant equations have the form $d(X \pm iY)/dt = (X \pm iY)f_{1\pm} + (X \mp iY)^3 f_{2\pm}$, $dZ/dt = f_Z$, where the functions $f_{1\pm}$, $f_{2\pm}$, f_Z depend only on the invariants $X^2 + Y^2$, $X^4 - 6X^2Y^2 + Y^4$, $4X^3Y - 4XY^3$. These equations, and the image equations without symmetry, have previously been described [1,3].

For the group \mathcal{V}_4 none of the three variables X, Y, Z transforms under the identity representation. The most general three-dimensional system equivariant under \mathcal{V}_4 has the form

$$\frac{d}{dt} \begin{bmatrix} X \\ Y \\ Z \end{bmatrix} = \begin{bmatrix} \alpha_1 X + \beta_1 YZ \\ \alpha_2 Y + \beta_2 ZX \\ \alpha_3 Z + \beta_3 XY \end{bmatrix}. \quad (1)$$

The coefficients α_i , β_i are generally functions of the four invariant polynomials X^2 , Y^2 , Z^2 , XYZ .

For \mathcal{V}_4 a $4 \rightarrow 1$ local diffeomorphism that maps each of the four domains in $\mathbb{R}^3(X, Y, Z)$ onto $\mathbb{R}^3(u_1, u_2, u_3)$ is given by the transformation

$$\begin{aligned} u_1 &= \frac{1}{2}(X^2 - Y^2), \\ u_2 &= \frac{1}{2}(X^2 + Y^2 - 2Z^2), \\ u_3 &= XYZ. \end{aligned} \quad (2)$$

The image (or reduced) dynamical equations are

$$\frac{d}{dt} \begin{bmatrix} u_1 \\ u_2 \\ u_3 \end{bmatrix} = \frac{\partial u_i}{\partial X_j} \frac{dX_j}{dt} = \begin{bmatrix} X & -Y & 0 \\ X & Y & -2Z \\ YZ & ZX & XY \end{bmatrix} \begin{bmatrix} \alpha_1 X + \beta_1 YZ \\ \alpha_2 Y + \beta_2 ZX \\ \alpha_3 Z + \beta_3 XY \end{bmatrix}. \quad (3)$$

The Jacobian is noninvertible on the singular set

$$\det \left[\frac{\partial u_i}{\partial X_j} \right] = 2(X^2 Y^2 + Y^2 Z^2 + Z^2 X^2) = 0. \quad (4)$$

This set is the union of the three rotation axes: the X , Y , and Z axes.

The image equations are obtained by multiplying out the matrices or the right hand side of Eq. (3), for example,

$$\frac{du_1}{dt} = \alpha_1 X^2 - \alpha_2 Y^2 + (\beta_1 - \beta_2) XYZ. \quad (5)$$

However, the equivariant variables must be expressed in terms of the new invariant variables u_1, u_2, u_3 . This is generally not possible until a fourth invariant is introduced: $r_4 = \frac{1}{2}(X^2 + Y^2 + Z^2)$. The three invariants X^2, Y^2, Z^2 are linearly related to u_1, u_2, r_4 :

$$\frac{1}{2} \begin{bmatrix} X^2 \\ Y^2 \\ Z^2 \end{bmatrix} = \frac{1}{6} \begin{bmatrix} 3 & 1 & 2 \\ -3 & 1 & 2 \\ 0 & -2 & 2 \end{bmatrix} \begin{bmatrix} u_1 \\ u_2 \\ r_4 \end{bmatrix}. \quad (6)$$

The equation of motion for u_1 is

$$\begin{aligned} \frac{du_1}{dt} &= (\alpha_1 + \alpha_2)u_1 + \frac{1}{3}(\alpha_1 - \alpha_2)u_2 + (\beta_1 - \beta_2)u_3 \\ &+ \frac{2}{3}(\alpha_1 - \alpha_2)r_4. \end{aligned} \quad (7)$$

The invariant polynomials X^2, Y^2, Z^2, XYZ satisfy a sixth-degree equation (“syzygy”)

$$(X^2)(Y^2)(Z^2) - (XYZ)^2 = 0. \quad (8)$$

As a result, the radical r_4 (second degree in X, Y, Z) satisfies a cubic equation, which is

$$2[(u_2 + r_4)^2 - 9u_1^2](r_4 - u_2) = 27u_3^3. \quad (9)$$

This means that the most general equations for the u_i have the form

$$\frac{du_i}{dt} = \sum_{r=0}^2 f_{ir}(u_1, u_2, u_3)r_4^r. \quad (10)$$

The fact that invariant images of equivariant equations generally depend on radical functions (e.g., r_4) which are solutions of nontrivial polynomial equations has greatly impeded

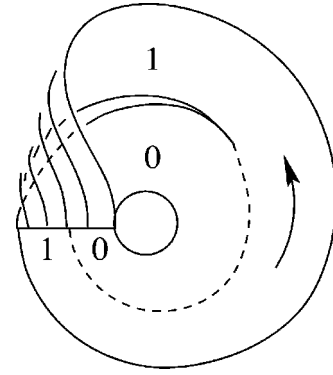


FIG. 2. Smale horseshoe branched manifold.

the study of how covering dynamical systems can be constructed from dynamical systems without symmetry.

In $\mathbb{R}^3(X, Y, Z)$, the singular set of the group \mathcal{C}_4 is the Z axis, while that of \mathcal{V}_4 is the union of the X, Y , and Z axes. The image of the singular set of \mathcal{C}_4 in $\mathbb{R}^3(u_1, u_2, u_3)$ is the $u_3 = Z$ axis. The image of the singular set of \mathcal{V}_4 consists of three half-lines in the $u_3 = 0$ plane. These half-lines are

$$X \text{ axis, } u_1 = u_2 = \frac{1}{2}X^2 \geq 0, \quad u_3 = 0,$$

$$Y \text{ axis, } -u_1 = u_2 = \frac{1}{2}Y^2 \geq 0, \quad u_3 = 0,$$

$$Z \text{ axis, } u_2 = -Z^2 \leq 0, \quad u_1 = u_3 = 0.$$

As long as the image attractor does not intersect the image of the singular set in $\mathbb{R}^3(u_1, u_2, u_3)$, its lift under the inverse of the transformation (3) is structurally stable. This means that there is no change either in the number of periodic orbits or in their topological organization under a perturbation of the rotation axes.

V. DESCRIPTION OF STRANGE ATTRACTORS

Strange attractors in \mathbb{R}^3 can be described and classified by their branched manifolds [4]. The branched manifold that describes a common chaos-generating mechanism, the stretch-and-fold mechanism that creates a Smale horseshoe, is shown in Fig. 2. This mechanism is frequently encountered in physical systems. In particular, the Rössler dynamical system exhibits this mechanism for some parameter values.

This particular branched manifold has two branches, labeled 0 and 1, and one branch line. The branch line is partitioned into two subintervals labeled 0 and 1. Initial conditions on segment 0 of the branch line flow through branch 0 back to the full branch line; similarly for initial conditions on the interval 1. The flow properties are summarized by a transition matrix T_{ij} , where i indexes intervals of the branch line that act as initial conditions for the flow through branch i . For the branched manifold shown in Fig. 2,

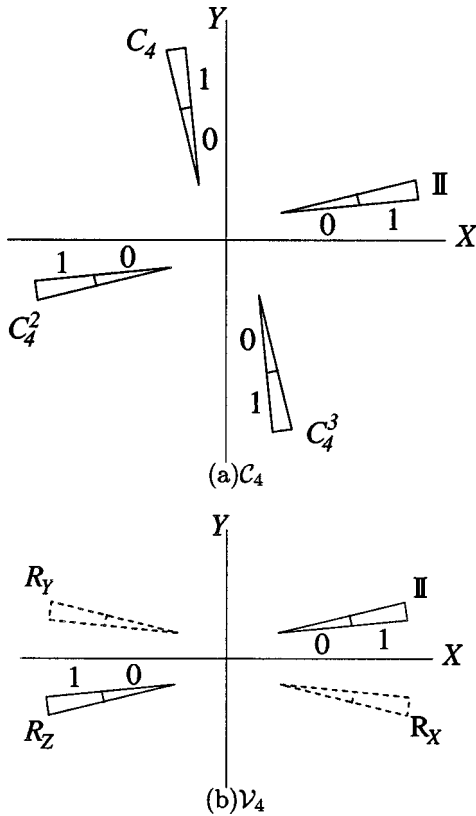


FIG. 3. Possible arrangement of the branch lines in two different fourfold covers of the Smale horseshoe branched manifold. (a) \mathcal{C}_4 , (b) \mathcal{V}_4 . In (b), dashed lines indicate that the branch line is below the $Z=0$ plane. The width increases with distance from this plane.

$$T = \begin{matrix} & 0 & 1 \\ 0 & \begin{bmatrix} 1 & 1 \\ 1 & 1 \end{bmatrix} \\ 1 & \end{matrix} \quad (11)$$

Fourfold covers of branched manifolds with b branch lines and n branches have $4b$ branch lines and $4n$ branches. The $4b$ branch lines and $4n$ branches are mapped into each other by the operations of the symmetry group. In Fig. 3(a) we show how the four branch lines of a fourfold cover of the Smale horseshoe manifold may be organized in a structurally stable fourfold cover. One branch line is completely contained in the fundamental domain $\mathbb{I} = (+++) \cup (++-)$. The other three branch lines are completely contained in the other three domains, and can be labeled by an appropriate group operation. In Fig. 3(b) we show a possible arrangement of the branch lines in a fourfold cover with \mathcal{V}_4 symmetry of the Smale horseshoe branched manifold when one branch line occurs in the positive octant $(+++)$ of the fundamental domain $\mathbb{I} = (+++) \cup (---)$.

The transition matrices describing the flow in the fourfold covering branched manifold are 8×8 matrices. These matrices are completely determined from a limited amount of information. Specifically, we must specify the destination (i.e., branch) of flows whose sources are in the branch intervals in

the fundamental domain. We give one example each for \mathcal{C}_4 and \mathcal{V}_4 invariant fourfold covers.

Example \mathcal{C}_4 . Assume that points in $0(\mathbb{I})$ flow back to the branch labeled \mathbb{I} , while points in $1(\mathbb{I})$ flow to the next branch, labeled \mathcal{C}_4 . Branch \mathbb{I} is mapped to the remaining three branches by the three group operations $\mathcal{C}_4, \mathcal{C}_4^2, \mathcal{C}_4^3$. As a result,

$$\begin{aligned} 0(\mathcal{C}_4) &\rightarrow \mathcal{C}_4, & 1(\mathcal{C}_4) &\rightarrow \mathcal{C}_4^2, \\ 0(\mathcal{C}_4^2) &\rightarrow \mathcal{C}_4^2, & 1(\mathcal{C}_4^2) &\rightarrow \mathcal{C}_4^3, \\ 0(\mathcal{C}_4^3) &\rightarrow \mathcal{C}_4^3, & 1(\mathcal{C}_4^3) &\rightarrow \mathcal{C}_4^4 = \mathbb{I}. \end{aligned}$$

The transition matrix for this cover is

		\mathbb{I}		\mathcal{C}_4		\mathcal{C}_4^2		\mathcal{C}_4^3	
		0	1	0	1	0	1	0	1
\mathbb{I}	0	1	1	0	0	0	0	0	0
	1	0	0	1	1	0	0	0	0
\mathcal{C}_4	0	0	0	1	1	0	0	0	0
	1	0	0	0	0	1	1	0	0
\mathcal{C}_4^2	0	0	0	0	0	1	1	0	0
	1	0	0	0	0	0	0	1	1
\mathcal{C}_4^3	0	0	0	0	0	0	0	1	1
	1	1	1	0	0	0	0	0	0

(12)

Example \mathcal{V}_4 . In this example, we assume $0(\mathbb{I}) \rightarrow \mathcal{R}_X$ and $1(\mathbb{I}) \rightarrow \mathcal{R}_Y$. The full flow information is obtained by moving the branch line in the fundamental domain to the other three branch lines using the other three group operations:

$$0(\mathbb{I}) \rightarrow \mathcal{R}_X, \quad 1(\mathbb{I}) \rightarrow \mathcal{R}_Y,$$

$$\mathcal{R}_X: 0(\mathcal{R}_X) \rightarrow \mathcal{R}_X \mathcal{R}_X = \mathbb{I}, \quad 1(\mathcal{R}_X) \rightarrow \mathcal{R}_X \mathcal{R}_Y = \mathcal{R}_Z,$$

$$\mathcal{R}_Y: 0(\mathcal{R}_Y) \rightarrow \mathcal{R}_Y \mathcal{R}_X = \mathcal{R}_Z, \quad 1(\mathcal{R}_Y) \rightarrow \mathcal{R}_Y \mathcal{R}_Y = \mathbb{I},$$

$$\mathcal{R}_Z: 0(\mathcal{R}_Z) \rightarrow \mathcal{R}_Z \mathcal{R}_X = \mathcal{R}_Y, \quad 1(\mathcal{R}_Z) \rightarrow \mathcal{R}_Z \mathcal{R}_Y = \mathcal{R}_X.$$

The transition matrix is easily constructed using this information. It is transparent when expressed in terms of the ‘‘dressed symbols.’’ These are the symbols required to describe the dynamics in the image attractor dressed with the operations in the group \mathcal{G} :

σ_i		0				1				
	g_α	I	R_X	R_Y	R_Z	I	R_X	R_Y	R_Z	
0	I	0	1	0	0	0	1	0	0	
	R_X	1	0	0	0	1	0	0	0	
	R_Y	0	0	0	1	0	0	0	1	
	R_Z	0	0	1	0	0	0	1	0	
1	I	0	0	1	0	0	0	1	0	
	R_X	0	0	0	1	0	0	0	1	
	R_Y	1	0	0	0	1	0	0	0	
	R_Z	0	1	0	0	0	1	0	0	

	0	1
$\rightarrow 0$	$\Gamma^{\text{Reg}}(R_X)$	$\Gamma^{\text{Reg}}(R_X)$
1	$\Gamma^{\text{Reg}}(R_Y)$	$\Gamma^{\text{Reg}}(R_Y)$

(13)

It is clear from this that the entire transition matrix can be constructed from the diagonal blocks. The 16 distinct transition matrices for the equivariant covers of the Smale horseshoe are

	0	1
$T(0 \rightarrow g_\alpha, 1 \rightarrow g_\beta) = 0$	$\Gamma^{\text{Reg}}(g_\alpha)$	$\Gamma^{\text{Reg}}(g_\alpha)$
1	$\Gamma^{\text{Reg}}(g_\beta)$	$\Gamma^{\text{Reg}}(g_\beta)$

(14)

with $1 \leq \alpha, \beta \leq 4$. These results are easily extended when more symbols are required, to other groups and to covers where the image attractor has more than one branch line [4].

In Fig. 4 we show three projections of a cover of the Rössler attractor that has \mathcal{V}_4 symmetry. This cover is structurally stable and is defined by the index $0 \rightarrow I, 1 \rightarrow R_X$. This cover has two components. Only the component with branch lines in domain R_Y and R_Z is shown.

VI. LIFTS OF PERIODIC ORBITS

Periodic orbits embedded in an image strange attractor lift to periodic orbits in its covering strange attractors. An orbit of period p in the horseshoe attractor lifts to an orbit of period $p, 2p$, or $4p$ in any fourfold cover. We illustrate with a few examples.

Example 1. The orbit 101 lifts to two period-6 orbits in the fourfold cover with C_4 symmetry described by the transition matrix (12). To show this, we repeat the symbol sequence 101 several times, and dress each symbol with two labels. The first label identifies the source branch, the second identifies the sink (e.g., $0_{(I,I)}, 0_{(C_4,C_4)}, 1_{(I,C_4)}$, etc.). Beginning on the branch I, we find

$$1_{(I,C_4)} 0_{(C_4,C_4)} 1_{(C_4,C_4)} 1_{(C_4,C_4)} 0_{(C_4,C_4)} 1_{(C_4,C_4)} 1_{(C_4,I)}. \quad (15a)$$

The second label of symbol i must be the same as the first label of the next symbol $i + 1$. As a result, dressed symbolic dynamics is equivalent to matrix multiplication by the submatrices on the diagonal blocks of the transition matrices expressed in terms of the dressed symbols. The lift of 101 closes after $2 \times 3 = 6$ periods (symbols), when the first group

label in this sequence is equal to the last. A second, distinct but symmetry related lift of 101 is

$$1_{(C_4,C_4)} 0_{(C_4,C_4)} 1_{(C_4,C_4)} 1_{(C_4,I)} 0_{(I,I)} 1_{(I,C_4)}. \quad (15b)$$

Thus, 101 is covered by two period-6 orbits in the fourfold cover defined by the transition matrix (12). By similar arguments, 1011 lifts to a single period-16 orbit in this fourfold cover.

Example 2. The orbit 101 lifts to two period-6 orbits in the fourfold cover, with \mathcal{V}_4 symmetry defined by the transition matrix (13). By using the arguments of Example 1, we compute

$$1_{(I,R_Y)} 0_{(R_Y,R_Z)} 1_{(R_Z,R_X)} 1_{(R_X,R_Z)} 0_{(R_Z,R_Y)} 1_{(R_Y,I)}, \quad (16a)$$

$$1_{(R_Y,I)} 0_{(I,R_X)} 1_{(R_X,R_Z)} 1_{(R_Z,R_X)} 0_{(R_X,I)} 1_{(I,R_Y)}. \quad (16b)$$

Remark. The matrix elements that occur in the computations above occur in faithful representations of specific group operations. For example, in the \mathcal{V}_4 symmetric cover with transition matrix (13), the symbols 0,1 are represented by 4×4 matrices

$$0 \rightarrow \begin{matrix} I \\ R_X \\ R_Y \\ R_Z \end{matrix} \begin{bmatrix} 0 & 1 & 0 & 0 \\ 1 & 0 & 0 & 0 \\ 0 & 0 & 0 & 1 \\ 0 & 0 & 1 & 0 \end{bmatrix}, \quad 1 \rightarrow \begin{matrix} I \\ R_X \\ R_Y \\ R_Z \end{matrix} \begin{bmatrix} 0 & 0 & 1 & 0 \\ 0 & 0 & 0 & 1 \\ 1 & 0 & 0 & 0 \\ 0 & 1 & 0 & 0 \end{bmatrix}. \quad (17)$$

These matrices are faithful representations for the action of R_X (for 0) and R_Y (for 1) on the four domains in $\mathbb{R}^3(X, Y, Z)$. As a result, information about the periodicity of orbits covering a period p orbit can be reduced to a product of group operations, as follows:

$$C_4 \ 101 \rightarrow \begin{matrix} C_4 & I & C_4 & C_4 & I & C_4 & \cdots \\ C_4 & C_4 & C_4^2 & C_4^3 & C_4^3 & I & \cdots \end{matrix}$$

In the top line we replace each symbol by its group label [cf. (15a)]. Below this we provide the cumulative product. The computations become simpler if we assign a group value to

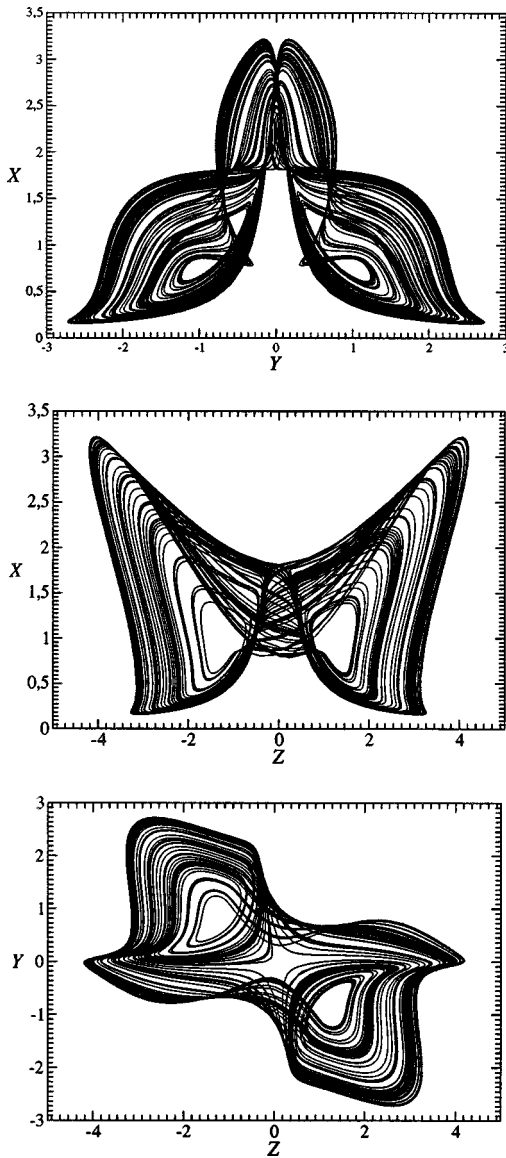


FIG. 4. Cover of the Rössler attractor with \mathcal{V}_4 symmetry. The index is $\{0 \rightarrow I, 1 \rightarrow R_X\}$. Two disconnected covers exist. The one shown here connects branch lines labeled R_Y and R_Z . Its partner connects the branches labeled I and R_X .

the basic symbol sequence: $101 \rightarrow C_4 I C_4 = C_4^2$. Then $(101)^2 = I$. For the symbol sequence 1011, we have $1011 \rightarrow C_4 I C_4 C_4 = C_4^3$, so $(1011)^4$ is closed in the cover.

In the general case, covers of orbits of period p in an image attractor are obtained by writing out the symbol sequence. Each symbol is replaced by an appropriate group operation, given by the index of the cover. The product g_i is computed, and the smallest positive integer k with the property that $g_i^k = I$ is determined. There are $|\mathcal{G}|/k$ covering orbits of period kp in the covering attractor of the original orbit of period p in the image attractor.

For lifts with \mathcal{V}_4 symmetry, the group operation assigned to any symbol sequence in the image is either I or R_X, R_Y , or R_Z . In the first, case a period- p orbit lifts to four period-

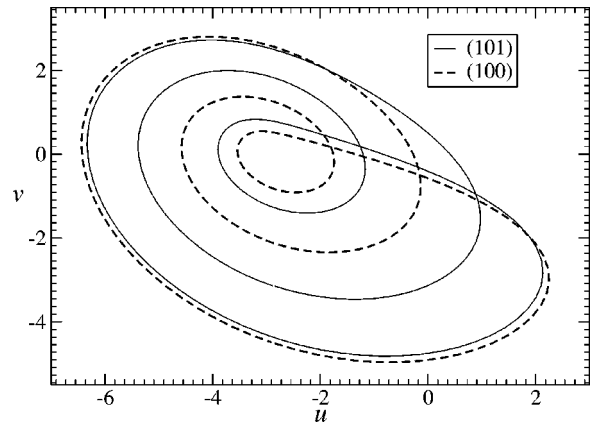


FIG. 5. Period-3 orbits embedded within the Rössler attractor.

p orbits. In the second case, a period- p orbit lifts to two period- $2p$ orbits. For example, $101 \rightarrow R_Y R_X R_Y = R_X$, so 101 lifts to a pair of period-6 orbits.

Remark. The symbol sequence in the orbit (15b) is closely related to the symbol sequence in orbit (15a); similarly for orbits (16b) and (16a). The general relation is as follows. Assign to any symbol sequence in the image its appropriate group operation g_i as described above. This group operation generates a subgroup $\mathcal{K} = \{g_i, g_i^2, \dots, I\}$. One orbit in the cover is obtained by starting in the fundamental domain and assigning group labels to the p symbols of the image orbit: $1, C_4^0, C_4, C_4^1, C_4^2$. If $g_i^1 \neq I$ the next p symbols are obtained by multiplying each of the group operations by g_i from the left. If $g_i^2 \neq I$, the next p symbols are obtained by multiplying by g_i^2 , etc. The symbolic names of symmetry-related orbits are obtained as follows. The subgroup \mathcal{K} partitions \mathcal{G} into cosets. For $g_i = C_4^2$ the two cosets of \mathcal{C}_4 are $\{I, C_4^2\}$ and $\{C_4, C_4^3\}$. The first orbit (15a) starting in the fundamental domain corresponds to choosing I as a coset representative. For the second orbit we choose a representative from the second coset: either C_4 or C_4^3 . If we choose C_4 , we multiply all group operations in the first orbit by C_4 on the left to obtain the symmetric orbit. This maps orbit (15a) to (15b). If we choose the other group operator C_4^3 as the coset representative, this corresponds to starting the symbol sequence at the second triple [fourth symbol in orbit (15b)]. For the orbits (16), $g_i = R_X$ and the cosets are $\{I, R_X\}$ and $\{R_Y, R_Z\}$. The coset representatives chosen are I for orbit (16a) and R_Y for orbit (16b). Choosing R_Z instead of R_Y as the second coset representative initiates orbit (16b) at the fourth symbol.

In Fig. 5 we show the period-3 saddle 101 and its partner node 100 in the Rössler attractor. They are lifted to covering orbits in the cover with \mathcal{V}_4 symmetry and indices $0 \rightarrow R_Y, 1 \rightarrow R_Z$. Figure 6(a) shows the two period-6 covers of the node (100) in the covering attractor. Since $100 \rightarrow R_Z R_Y R_Y = R_Z$, evolution during three periods maps a point on this orbit in domain I to its image under R_Z in domain R_Z (solid line). Since $R_Z^2 = I$, this cover orbit has period 6. The partner period-6 orbit is shown dashed. It is obtained from the solid curve by operations R_Y or R_X . In Fig. 6(b) we show lifts of

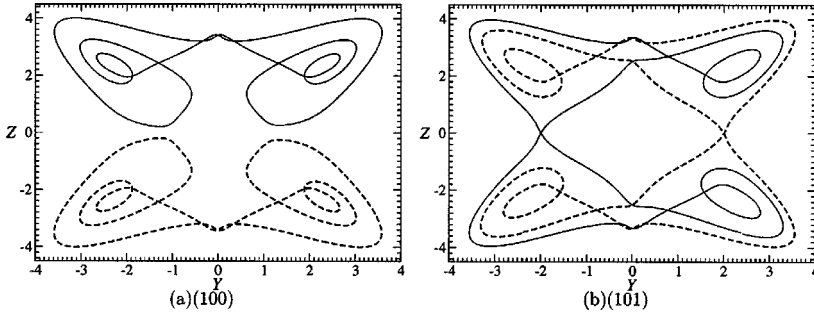


FIG. 6. \mathcal{V}_4 -fold cover with indexes $0 \rightarrow R_Y, 1 \rightarrow R_Z$ of the period-3 orbits shown in Fig. 5. Covers of (a) (100), (b) (101). In both cases the covers consist of two symmetry-related period-6 orbits.

the saddle partner 101. For this orbit, $101 \rightarrow R_Z R_Y R_Z = R_Y$. By a similar reason, there are two period-6 orbits covering 101. One maps I to R_Y after three periods (solid). The dashed curve is obtained by rotating the solid curve by R_X or R_Z . We remark that the covering attractor is structurally stable and consists of one component, but covers of any orbit of period p in the Rössler attractor consist either of four orbits of period p or two of period $2p$ (not one of period $4p$).

VII. SPECTRUM OF COVERS

An equivariant cover of a strange attractor is defined by the group label assigned to each symbol and is used to label orbits in the image attractor. For a strange attractor classified by a branched manifold with two branches, there are $|\mathcal{G}|^2$ structurally stable covers with $|\mathcal{G}|$ -fold symmetry. For the symmetry group C_4 , these 16 distinct C_4 -invariant covers are organized as follows:

	Symbol			Group labels
C_4	0	I	$\left \begin{array}{ccc} \text{I} & C_4^2 & C_4^2 \\ C_4^2 & \text{I} & C_4^2 \end{array} \right $	$\text{I} \ C_4 \ \text{I} \ C_4^3 \ C_4 \ C_4^2 \ C_4 \ C_4^3 \ C_4^2 \ C_4^3 \ C_4 \ C_4^3$
	1	I		$C_4 \ \text{I} \ C_4^3 \ \text{I} \ C_4^2 \ C_4 \ C_4^3 \ C_4 \ C_4^3 \ C_4^2 \ C_4 \ C_4^3$
		Four components	Two components	Connected covers

The fourfold cover with index $(0,1) \rightarrow (\text{I}, \text{I})$ consists of four disconnected pieces. The cover with index $(0,1) \rightarrow (\text{I}, C_4^2)$ consists of two disconnected pieces. Two branch lines, I and C_4^2 , are in one component while the other two, C_4 and C_4^3 , lie in the other component. The cover with index $(0,1) \rightarrow (C_4^2, \text{I})$ is dual to that with index (I, C_4^2) . Duality is defined by exchanging the sinks for the two sources. The fourfold cover with index $(0,1) \rightarrow (C_4^2, C_4^2)$ also consists of two components. It is self-dual. The remaining 12 covers are connected. For each there is a path in the attractor from any branch line to any other branch line. These 12 are divided into five dual pairs $(C_4^i, C_4^j) \leftrightarrow (C_4^j, C_4^i), i \neq j, i, j$ both not even, and two self-dual covers $(C_4^i, C_4^i), i = 1, 3$.

The 16 fourfold covers of the Smale horseshoe branched manifold with \mathcal{V}_4 symmetry are partitioned as follows:

	Symbol		Index
\mathcal{V}_4	0	I	$\left \begin{array}{cccc} \text{I} & \text{I} & \text{I} & R_X \ R_Y \ R_Z \\ R_X \ R_Y \ R_Z & \text{I} & \text{I} & \text{I} \end{array} \right R_X \ R_Y \ R_Z \ R_X \ R_Z \ R_Y$
	1	I	$\left \begin{array}{cccc} R_X \ R_Y \ R_Z & \text{I} & \text{I} & \text{I} \\ R_Y \ R_Z \ R_X \ R_Z \ R_Y \ R_X \end{array} \right R_Y \ R_Z \ R_X \ R_Z \ R_Y \ R_X$
		Four components	Two components
			Connected covers

The cover $(0,1) \rightarrow (\text{I}, \text{I})$ consists of four disconnected components. The next nine consist of two disconnected components. There are three dual pairs, $(\text{I}, R_X) \leftrightarrow (R_X, \text{I})$, etc., and three self-dual covers, e.g., (R_X, R_X) . For example, the cover with index $(0,1) \rightarrow (\text{I}, R_Z)$ has one component containing branch lines I and R_Z , while the symmetry-related component (under either R_X or R_Y) contains branch lines R_X and R_Y . Similarly for the self-dual cover, $(0,1) \rightarrow (R_Z, R_Z)$. The three covers with indices $(\text{I}, R_X), (\text{I}, R_Y), (\text{I}, R_Z)$ are related to each other by rotations about the $(1,1,1)$ axis by $2\pi/3$ radians, i.e., by the group C_3 .

The remaining six covers consist of a single connected component. There is a path in each of these branched manifolds from any branch line to any other branch line. There

are three dual pairs, such as $(R_X, R_Y) \leftrightarrow (R_Y, R_X)$. In addition, the first three $(R_X, R_Y), (R_Y, R_Z), (R_Z, R_X)$ are mapped into each other under C_3 , as are the last three in this list. If we regard the symmetry-related attractors (under C_3) as essentially equivalent, the breakdown of distinct \mathcal{V}_4 -invariant covers of Smale horseshoe dynamics is

No. of components	No. of dual pairs	No. of self-dual pairs
4	0	1 (I, I)
2	1 (I, R_X)	1 (R_X, R_X)
1	1 (R_X, R_Y)	0

In summary, there are six $[=2 \times (0+1+1)+1 \times (1+1+0)]$ topologically distinct types of fourfold covers of the basic Smale horseshoe branched manifold with \mathcal{V}_4 symmetry.

For covers with four components, lifts of period- p orbits consist of four disjoint period- p orbits, one in each component. For covers with two components, lifts of period- p orbits can be of period p or $2p$. For connected covers, lifts can be of period p (four of them) or $2p$ (two of them), but there can be no orbits of period $4p$. This is true because any orbit of period p is assigned one of the four symbols \mathbb{I} , or R_X, R_Y, R_Z . In the first case $\mathbb{I}^k = \mathbb{I}, k=1$, so the cover has period p . In the second case $R_X^2 = \mathbb{I}$ (similarly for R_Y, R_Z), so $k=2$ and the two covers have period $2p$. This is illustrated in Fig. 6. This clarifies the mystery reported in Ref. [7] that covering orbits of period $4p$ are not observed in a connected structurally stable strange attractor with \mathcal{V}_4 symmetry.

Observation. In any of the equivariant covers described above, the branch lines that can be reached from the branch line in the fundamental domain are exactly those labeled by group elements that can be obtained by multiplying the symbol indices in all possible orders. To put this another way, the symbol indices are generators of a subgroup $\mathcal{H} \subseteq \mathcal{G}$. One component of the equivariant cover contains exactly the branch lines labeled by the elements of the subgroup \mathcal{H} . There are $|\mathcal{G}|/|\mathcal{H}|$ components in the equivariant cover. These components can be labeled by the coset representatives of \mathcal{G}/\mathcal{H} .

VIII. STRUCTURALLY UNSTABLE COVERS

When the image of the singular set in $\mathbb{R}^3(u_1, u_2, u_3)$ intersects the image attractor, the singular set intersects the equivariant covering attractor in $\mathbb{R}^3(\mathbf{X})$. The intersection has absolutely no effect on the image attractor but a profound effect on the covering attractor. To be precise, the covering attractor is structurally unstable. A perturbation of the location of the intersection changes the periodicity, structure, and organization of many unstable periodic orbits in the cover. The bifurcation due to this structural instability has been named the peeling bifurcation [1].

In the structurally unstable case, the flow from one of the intervals of the branch line in the fundamental domain is split into components that flow to two different branch lines in adjacent domains. As an example, we consider a cover of the Smale horseshoe branched manifold with \mathcal{V}_4 symmetry and index $(0,1) \rightarrow (\mathbb{I}, R_Y)$. This cover has two disconnected components. Now we displace the image attractor so that branch 0 intersects the image of the Z axis $u_1 = u_3 = 0, u_2 \leq 0$. Then the flow from $0(\mathbb{I})$ is split between the branch line in the fundamental domain and the domain R_Z . There is a

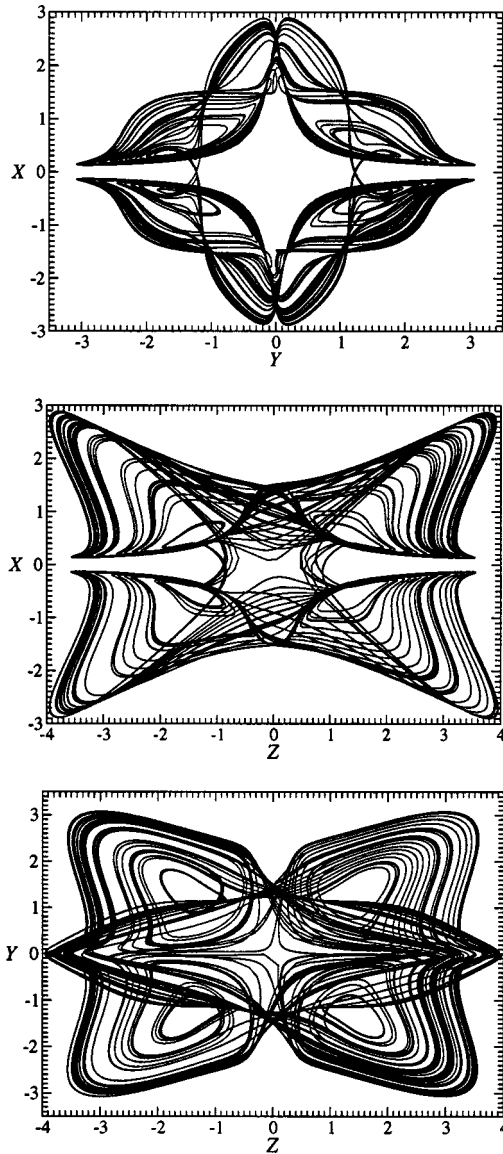


FIG. 7. Structurally unstable cover of the Rössler attractor with \mathcal{V}_4 symmetry. The index is $(0,1) \rightarrow (\mathbb{I}, R_Y + R_Z)$.

path from branch line \mathbb{I} to every other branch line. As a result, the structurally unstable attractor is now connected. It is labeled by the index $(0,1) \rightarrow (\mathbb{I}, R_Z + R_Y)$. After the $u_2 \leq 0$ axis passes through branch 0 to the space between the two branches, the cover becomes once again structurally stable, has index $(0,1) \rightarrow (R_Z, R_Y)$, and is connected. The intersection of the half axis $u_1 = u_3 = 0, u_2 \leq 0$ with branch 0 causes a global symmetry-restoring bifurcation. In this case the bifurcation is summarized by

Index $(0 \rightarrow \mathbb{I}, 1 \rightarrow R_Y)$	$(0 \rightarrow \mathbb{I} + R_Z, 1 \rightarrow R_Y)$	$(0 \rightarrow R_Z, 1 \rightarrow R_Y)$	(18)
structurally stable	structurally unstable	structurally stable	

Remark. In structurally unstable cases the flow is split between branch lines in adjacent domains (Fig. 1). The connectivity of the structurally unstable cover is determined by computing the subgroup \mathcal{H} , now using all appropriate group labels. For example, \mathcal{H} for $(0,1) \rightarrow (\mathbb{I}, R_Y)$ is generated by \mathbb{I} and R_Y and is the two-element group $\mathcal{H} = \{\mathbb{I}, R_Y\}$, whereas in the structurally unstable case $(0,1) \rightarrow (\mathbb{I}, R_Y + R_Z)$, \mathcal{H} is generated by \mathbb{I} , R_Z , R_Y and consists of all four group operations: $\mathcal{H} = \{\mathbb{I}, R_X, R_Y, R_Z\} = \mathcal{G}$. In this case, $|\mathcal{G}|/|\mathcal{H}| = 1$ shows that the cover has one connected component. A connected structurally unstable cover with index $(\mathbb{I}, R_Y + R_Z)$ is shown in Fig. 7.

IX. REMARKS, SUMMARY, AND CONCLUSIONS

Strange attractors with no symmetry can be lifted to strange attractors with symmetry group \mathcal{G} . Many distinct inequivalent strange attractors, all with the same image, can be equivariant under the symmetry group \mathcal{G} .

If s symbols suffice to uniquely describe all the unstable periodic orbits in the image attractor, $|\mathcal{G}|s$ symbols are required to label the periodic orbits in any of the \mathcal{G} -equivariant covering strange attractors. The $|\mathcal{G}|s$ symbols are labeled by two indices: one is one of the s symbols necessary for symbolic dynamics in the image, the other is one of the $|\mathcal{G}|$ group operations in the symmetry group \mathcal{G} . There are $|\mathcal{G}|^s$ distinct covering strange attractors that are equivariant under \mathcal{G} with the same image attractor.

Symbolic dynamics in equivariant covers is easily carried out. Each symbol from the image picks up two labels: one indicates the source domain for the flow, the other indicates the target domain. Examples include $0(\mathbb{I}, C_4)$ and $1(R_X, R_Y)$. If the targets for sources in the fundamental domain are known, targets for sources in the remaining domains are determined by the group action. In fact, group operation pairs are matrix elements for faithful permutation (or regular) representations of the group action on the spatial domains. These matrices are used to construct the transition matrix for each distinct cover. They therefore can be used to identify the inequivalent covers. The identification is made by an index: the index is an assignment of a group operation $g_\alpha \in \mathcal{G}$ to each symbol σ_i in the symbol set for the image attractor, $\sigma_i \rightarrow g_{\alpha_i}$.

Once an index is assigned, the structure and properties of the equivariant cover are determined. The group operations in the index generate a subgroup $\mathcal{H} \subseteq \mathcal{G}$. The number of dis-

connected components in the equivariant cover is $|\mathcal{G}|/|\mathcal{H}|$. If there is more than one component, they are labeled by coset representatives in \mathcal{G}/\mathcal{H} . The set of branch lines in the connected component containing the branch line in the fundamental domain are labeled by the group elements of \mathcal{H} . The structure of the remaining $|\mathcal{G}|/|\mathcal{H}| - 1$ components are determined by multiplying \mathcal{H} by the coset representatives.

Covers of orbits of period p in the image attractor are obtained by writing out the symbol sequence (e.g., 101). Each symbol is replaced by its index [e.g., (101) $\rightarrow R_Y R_X R_Y$ when the index is $(0,1) \rightarrow (R_X, R_Y)$] and the product is taken to determine a group operation $g_i \in \mathcal{G}$. This single group operator generates a subgroup $\mathcal{K} \subseteq \mathcal{H}$ of order k defined by the relation $g_i^k = \mathbb{I}$. An image orbit of period p lifts to $|\mathcal{H}/\mathcal{K}|$ orbits of period $p|\mathcal{K}|$ in each of the $|\mathcal{G}/\mathcal{H}|$ disconnected components of the \mathcal{G} -equivariant covering attractor.

Clearly, the structure of the group \mathcal{G} has a major influence on the spectrum and properties of \mathcal{G} -equivariant covering attractors. We have indicated these differences by using two groups of order four as examples. One has one generator, the other has two generators. Many group results are immediate: for example, if \mathcal{G} has two generators but $s > 2$, no connected structurally stable \mathcal{G} -equivariant covers are possible. If \mathcal{H} has two generators then $|\mathcal{H}/\mathcal{K}| > 1$, so that each component of an equivariant attractor contains at least two distinct disconnected orbits that cover an image orbit. If the invariant set of \mathcal{G} has too large a dimension (e.g., σ_Z in \mathbb{R}^3), index assignment is restricted and connected covering attractors are not possible.

Distinct covers exhibit dualities and may exhibit geometric equivalence. Structurally unstable covers involve group labels from adjacent spatial domains. Adjacency information is summarized in an ‘‘adjacency diagram’’ (Fig. 1).

These results are independent of the dimension of the dynamical system, even though all results have been illustrated on three-dimensional dynamical systems. The results depend on the symbolic dynamics in the image attractor and the structure of the equivariance group \mathcal{G} . Although the results have been illustrated for commutative groups \mathcal{G} , they hold without modifications for noncommutative groups as well.

ACKNOWLEDGMENTS

R.G. is supported in part by NSF Grant No. PHY 9987468. A part of this work was done during a stay by C.L. at Drexel University.

-
- [1] C. Letellier and R. Gilmore, *Phys. Rev. E* **63**, 016206 (2001).
 [2] C. Letellier and G. Gouesbet, *J. Phys. II* **6**, 1615 (1996).
 [3] R. Miranda and E. Stone, *Phys. Lett. A* **178**, 105 (1993).
 [4] R. Gilmore and M. Lefranc, *The Topology of Chaos* (Wiley, New York, 2002).

- [5] M. Hamermesh, *Group Theory and its Application to Physical Problems* (Dover, New York, 1989).
 [6] J.-M. Malasoma and M.-A. Boiron (unpublished).
 [7] J.-M. Malasoma, P. Werny, and M.-A. Boiron, *Chaos, Solitons Fractals* **15**, 487 (2002).